A Comprehensive Spectral Theory of Zonal-Mode Dynamics in Trapped Electron Mode Turbulence

P.W. Terry 1), R. Gatto 2), D.A. Baver 1), and E. Fernandez 3)

1) Department of Physics, University of Wisconsin-Madison, Madison, Wisconsin 53706
2) Dipartimento di Fisica, Universita' di Roma "Tor Vergata"
3) Eckerd College, St. Petersburg, Florida 33711

e-mail contact of main author: pwterry@wisc.edu

Abstract. A comprehensive, self-consistent theory for spectral dynamics in trapped electron mode (TEM) turbulence offers critical new understanding and insights into zonal-mode physics. This theory shows that 1) zonal mode structure, anisotropy, excitation, and temporal behavior arise at and from the interface of nonlinear advection and linear wave properties; 2) waves induce a marked spectral energy-transfer anisotropy that preferentially drives zonal modes relative to non zonal modes; 3) triplet correlations involving density (as opposed to those involving only flow) mediate the dominant energy transfer at long wavelengths; 4) energy transfer becomes inverse in the presence of wave anisotropy, where otherwise it is forward; 5) zonal-mode excitation is accompanied by excitation of a spectrum of damped eigenmodes, making zonal modes nonlinearly damped; and 6) the combination of anisotropic transfer to zonal modes and their nonlinear damping make this the dominant saturation mechanism for TEM turbulence. This accounts for the reduction of turbulence level by zonal modes, not zonal-flow E×B shearing.

1. Introduction

Zonal flows have been recognized as important in tokamak microturbulence on the basis of simulation results that show the level of turbulence rising by an order of magnitude when the coupling to zonal flows is artificially removed [1]. Zonal flows are thus thought to limit anomalous transport in tokamaks. Zonal flows are part of the fluctuation spectrum, originally postulated to form as the spectral condensate of the inverse cascade associated with the enstrophy-conserving vorticity advection nonlinearity [2]. However, all realistic models of tokamak microturbulence have advective nonlinearities involving scalars such as density and pressure. These nonlinearities produce forward cascades that dominate at large scales when the scalar evolves independently of the potential [3]. This paper examines how and why zonal flows are excited under such circumstances, and the properties of that excitation, using a simple model for trapped electron mode (TEM) turbulence. Spectral analysis treating the long wavelength nonlinearities comprehensively with relevant scalar fluctuations across the spectral compass establishes the mechanism by which zonal are saturated, their role in saturation of the turbulence and the mechanism by which it occurs, the role of damped eigenmodes in these processes (like the experimentally observed geodesic acoustic mode [4]), and the role of wave physics that dominates at long wavelengths. This analysis shows that there are strong links to the excitation of anisotropic large-scale structures in other kinds of turbulence [5]-[6].

2. Zonal Modes and Wave Anisotropy

Spectral energy transfer excites a significant zonal-mode spectrum feature in TEM turbulence. The process arises from TEM wave physics, as reflected in the fact that zonal modes constitute a global-scale spectrum structure whose anisotropy is determined by the wavenumber value that makes the wave frequency vanish [7]. This and other aspects of zonal mode excitation are robust features of the dynamical model [8]:

$$\frac{\partial n}{\partial t} - \nabla\phi \times \hat{\mathbf{z}} \cdot n + \upsilon(n - \phi) = -v_D \hat{\alpha} \frac{\partial \phi}{\partial y} \qquad (1)$$

$$\frac{\partial}{\partial t}(1-\nabla^2-\varepsilon^{1/2})\phi-\varepsilon^{1/2}\upsilon(n-\phi)+\nabla\phi\times\hat{\mathbf{z}}\cdot\nabla\nabla^2\phi=-v_D[1-\varepsilon^{1/2}\hat{\alpha}]\frac{\partial\phi}{\partial y} \quad . \qquad (2)$$

In this model $n = \varepsilon^{1/2}n_e + \phi$ is an effective electron density, n_e is the density of trapped electrons, ϕ is the potential, $\varepsilon^{1/2}$ is the trapping fraction, υ is the electron detrapping rate, v_D is the diamagnetic drift velocity, and $\hat{\alpha} = 1 + 3\eta_e/2$.

This paper addresses the collisionless regime, $\upsilon << v_D k_y$, in which the effective density and potential differ strongly. Therefore the density advection nonlinearity $\nabla\phi\times\mathbf{z}\cdot\nabla n$ is not small as it is in the collisional regime, but plays a significant role in the dynamics. This paper also addresses the long wavelength regime. There are two crucial features of the long wavelength regime. First, for $k < \sqrt{(n/\phi)_{rms}}$, the density advection nonlinearity dominates the spectral transfer rate ($\nabla\phi\times\mathbf{z}\cdot\nabla\nabla^2\phi$ plays a negligible role) because it has fewer spatial derivatives. This effect is accentuated by the fact that the deviation of density from the potential in the collisionless regime makes the density larger than the potential [8]. Second, the linear wave terms on the RHS of Eqs. (1) and (2) become dominant because they have one fewer spatial derivative than the density advection nonlinearity. In this regime spectral transfer necessarily involves the interaction of the density advection nonlinearity and the wave terms. The wave terms are fundamentally anisotropic, going as k_y. They induce strong anisotropy in spectral transfer and the fluctuation spectrum. In wave regimes with inverse transfer it has been shown that there is a singular layer in wavenumber space associated with the wavenumber for which the wave frequency vanishes [9]. The wave frequency, which is proportional to $v_D k_y$, cannot exceed the nonlinearities when it vanishes as $k_y \rightarrow 0$. Spectrally, this is a singular limit that forces a compensating enhancement of spectral density for $k_y \rightarrow 0$. This enhancement is the zonal mode spectrum [9].

In the collisionless, long wavelength regime, the dominance of density advection has been shown to produce a forward energy transfer associated with the violation of enstrophy invariance [3]. With zonal modes residing at long wavelengths, it is not obvious how they are driven in collisionless plasmas, particularly if unstable modes do not extend to very long wavelengths. However, in numerical solutions of Eqs. (1) and (2) zonal modes are observed to be strongly driven. This is illustrated in Fig. 1, which shows the spectral transfer rate as a function of k_x and k_y. The strong peaks represent absorption into zonal modes. The transfer in other parts of the spectrum is weaker. In this section we show that there is an isotropy of mode coupling that favors zonal mode excitation. In the final section we show that wave anisotropies induce inverse energy transfer. The anisotropy of coupling essentially represents an anisotropic spectral basin filled by the inverse transfer.

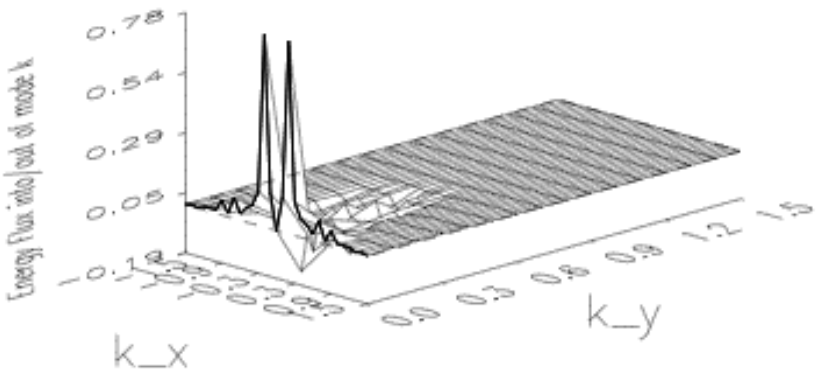

Fig. 1. Spectral energy transfer rate as a function of wavenumber. The strong peaks represent energy absorbed into the zonal modes by spectral transfer.

The anisotropy of mode coupling is clearly seen when the model is transformed via the eigenmode decomposition to obtain nonlinear evolution equations for the system's projection onto the basis set of linear eigenmodes [8]. The eigenmode decomposition is the proper way to deal with the fact that in turbulence with waves, time derivatives are an amplitude-dependent superposition of all eigenfrequencies, and not generally reducible to the frequency of the unstable mode, as commonly assumed. In the eigenmode decomposition Eqs. (1) and (2) can be written as [8]

$$\dot{\beta}_j(k) + i\omega_j\beta_j(k) = \sum_{k'} \frac{(-1)^j(\mathbf{k}'\times\hat{\mathbf{z}}\cdot\mathbf{k})i\upsilon\varepsilon^{1/2}}{[\omega_1(k)-\omega_2(k)](1+k^2-\varepsilon^{1/2})}[R_1(k')\beta_1(k')+R_2(k')\beta_2(k')]\beta_1(k-k') \ , \qquad (3)$$

where the subscript j takes on values 1 and 2, corresponding to the unstable and damped eigenmodes, β_j are the amplitudes, ω_j are the complex eigenfrequencies, and Rj are the eigenvectors specified as the ratio of density to potential at wavenumber k. The decomposition itself is given by $n_k = R_1(k)\beta_1(k) + R_2(k)\beta_2(k)$ and $\phi_k = \beta_1(k) + \beta_2(k)$. The eigenfrequencies and eigenvectors are obtained from a normal mode analysis of the linearization of Eqs. (1) and (2). The eigenfrequencies are given as roots of the dispersion relation $\omega^2(1+k^2-\varepsilon^{1/2}) + \omega[-v_D k_y(1-\hat{\alpha}\varepsilon^{1/2}) + i\upsilon(1+k^2)] - ik_y v_D\upsilon = 0$, and the eigenvectors as

$$R_j(k) = -\frac{(1+k^2-\varepsilon^{1/2})}{\upsilon\varepsilon^{1/2}}\left[i\omega_j - \frac{ik_y v_D(1-\hat{\alpha}\varepsilon^{1/2})+\upsilon\varepsilon^{1/2}}{1+k^2-\varepsilon^{1/2}}\right] \ . \qquad (4)$$

The mode coupling anisotropy that favors zonal modes resides in the factor $(\omega_1-\omega_2)^{-1}$. For $\upsilon/v_D k_y << 1$, $\omega_1 \approx v_D k_y(1-\hat{\alpha}\varepsilon^{1/2})/(1+k^2-\varepsilon^{1/2}) + \mathrm{O}(\upsilon)$, and $\omega_2 \approx -i\upsilon/(1-\hat{\alpha}\varepsilon^{1/2}) + \mathrm{O}(\upsilon^2/v_D k_y)$, from which is it seen that the difference $\omega_1-\omega_2$ goes as $v_D k_y$. As $k_y \to 0$, this difference drops by one order to $\mathrm{O}(\upsilon)$. Evaluation of $\omega_1-\omega_2$ for $k_y \to 0$ requires expansion of ω_1 and ω_2 in the limit $\upsilon/v_D k_y > 1$. Performing the expansion, this coupling factor is given by

$$\frac{1}{\omega_1-\omega_2} = \begin{Bmatrix} \dfrac{1+k^2-\varepsilon^{1/2}}{v_D k_y} & \text{for } k_y \neq 0 \\ \dfrac{i(1+k_x^2-\varepsilon^{1/2})}{\upsilon(1+k_x^2)} & \text{for } k_y = 0 \end{Bmatrix} \ , \qquad (5)$$

from which it is evident that coupling between zonal modes and non zonal modes is strongly enhanced over coupling purely between non zonal modes. Because zonal modes are not linearly driven, they represent available states in wavenumber space in which energy can accumulate via this coupling if there is energy available in the coupled modes k' and $k-k'$. When there is instability in adjacent parts of the spectrum this happens naturally as explained in the next section. If driven modes are removed in wavenumber space, inverse energy transfer is required.

The dominance of the electron density advection nonlinearity for long wavelengths $k < \sqrt{(n/\phi)_{rms}}$, means that the anisotropic spectral energy transfer that drives zonal modes resides primarily in the correlation $\langle n\phi n\rangle$, rather than the correlation $\langle \phi\phi\phi\rangle$. It is important that bispectrum observations seeking to verify zonal mode driving experimentally measure $\langle n\phi n\rangle$. Although the correlation $\langle \phi\phi\phi\rangle$ is a natural choice for flow structures, it is weaker when $k < \sqrt{(n/\phi)_{rms}}$.

3. Damped Eigenmode and Nonlinear Zonal Mode Damping

A crucial feature of Eq. (3) is that the damped eigenmode is nonlinearly driven at a rate identical to the rate of nonlinear absorption of instability energy. This follows because the

nonlinearity in the evolution equation of the unstable eigenmode is equal and opposite to the nonlinearity of the damped eigenmode equation. As the instability evolves toward saturation the former must become as large as the linear drive, which goes as $i\omega_1\beta_1$ and is growing exponentially in time. Because it has the same intensity, the nonlinearity of the damped eigenmode is much larger than the linear damping term, which is decaying exponentially. The nonlinearity therefore easily overcomes the damping and drives the damped eigenmode to finite amplitude. This is demonstrated in Fig. 2, which shows time histories of the energies of the unstable and damped eigenmodes from the numerical solution of Eq. (3). The damped eigenmode decays initially, and then, well before saturation, begins to grow exponentially. During its growth phase the evolution of the damped eigenmode is well described by parametric instability analysis [8].

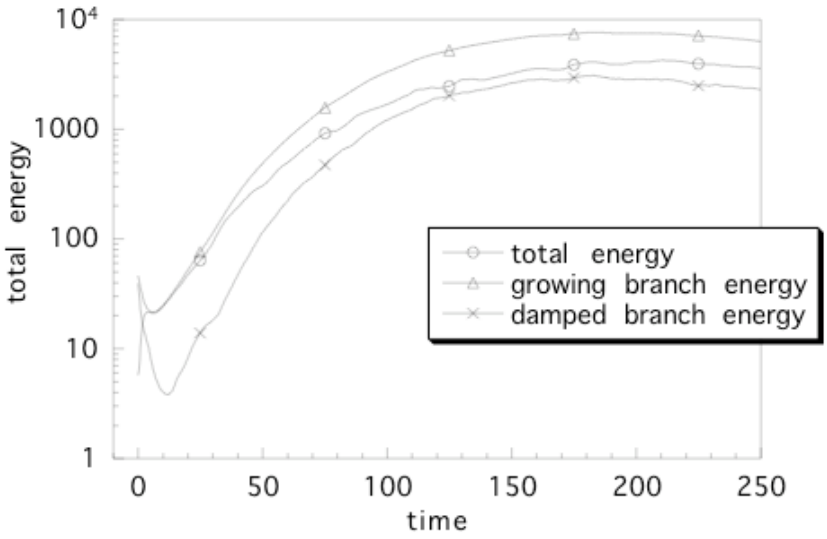

Fig. 2. Evolution of the energies in the unstable and damped eigenmodes.

With the excitation of the damped eigenmode the correlation of n and ϕ at finite amplitude is not given by the correlation of the linear instability, but by an amplitude-dependent superposition of the correlations of the instability and the damped eigenmode. The correlation of n and ϕ controls the rate at which energy is released into fluctuations by the free energy available in the gradients. Therefore the fluctuation-driving rate is not equal to the linear growth rate once the system reaches finite amplitude. The driving rate can be found from the rate of change of fluctuation energy. The fluctuation energy is defined as $W = \sum E(k) = \sum[(1+k^2-\varepsilon^{1/2})|\phi_k|^2 + \varepsilon^{1/2}|n_k|^2]$. Taking the time derivative of W and substituting from Eqs. (1) and (2) for the time derivatives of ϕ_k and n_k, the nonlinear terms vanish upon summation over k because W is an invariant of the nonlinearity. What remains is purely dissipative and represents the rate at which energy is injected into the spectrum or removed. Performing these operations the rate of change of energy is $dW/dt = \sum 2\gamma_k^{nl} E(k)$, where

$$\gamma_k^{nl} = \frac{k_y v_D \hat{\alpha}\varepsilon^{1/2}\,\mathrm{Im}\left\langle n_k^* \phi_k \right\rangle - \upsilon\varepsilon^{1/2}\left|(n_k - \phi_k)\right|^2}{(1+k^2-\varepsilon^{1/2})\left|\phi_k\right|^2 + \varepsilon^{1/2}\left|n_k\right|^2} \quad . \tag{6}$$

Although the conservative nonlinear transfer rates do not appear in Eq. (6), and products of amplitudes appear in both the numerator and denominator, this is an amplitude-dependent, or nonlinear, growth rate. When the linearly unstable eigenmode is used to write n in terms of ϕ, i.e., $n_k = R_1(k)\phi_k$, Eq. (6) reproduces the linear growth rate. However, if the fluctuations develop any other relationship between n and ϕ, as occurs with excitation of the damped eigenmode, γ^{nl} is different from the linear growth rate. The second term in the numerator of

the nonlinear growth rate is negative definite, hence instability occurs only if $\mathrm{Im}\langle n_k^* \phi_k \rangle$ is positive. With k_y=0 for zonal modes, the term with $\mathrm{Im}\langle n_k^* \phi_k \rangle$ vanishes, and the nonlinear growth rate is given by

$$\gamma_{k_x}^{nl} = \left. \frac{-\upsilon \varepsilon^{1/2} |(n_k - \phi_k)|^2}{(1 + k_x{}^2 - \varepsilon^{1/2}) |\phi_k|^2 + \varepsilon^{1/2} |n_k|^2} \right|_{k_y=0} . \qquad (7)$$

It is evident that at finite amplitude zonal modes are either damped or marginally stable, depending the values of n and ϕ. For k_y=0, the unstable eigenvector is R_1=1, yielding n_k=ϕ_k, and making γ^{nl} zero. This recovers the well-known result that zonal modes of the unstable drift wave are marginally stable. (It should be recalled that n is an effective density.) However, because the growth rate goes like $-|n_k - \phi_k|^2$, any deviation of the fluctuation structure from the eigenmode of the linear instability will cause the zonal modes to become damped. The excitation of the damped eigenmode is a significant deviation that causes the zonal modes to be robustly damped. Figure 3 shows the linear growth rate spectrum of the linear instability (on the left) and the growth rate at finite amplitude (on the right). The crease along k_y=0 in the linear spectrum has γ^{nl}=0 and represents the marginal stability of zonal modes on the unstable eigenmode branch. At finite amplitude the crease widens and deepens, becoming a significant sink of energy.

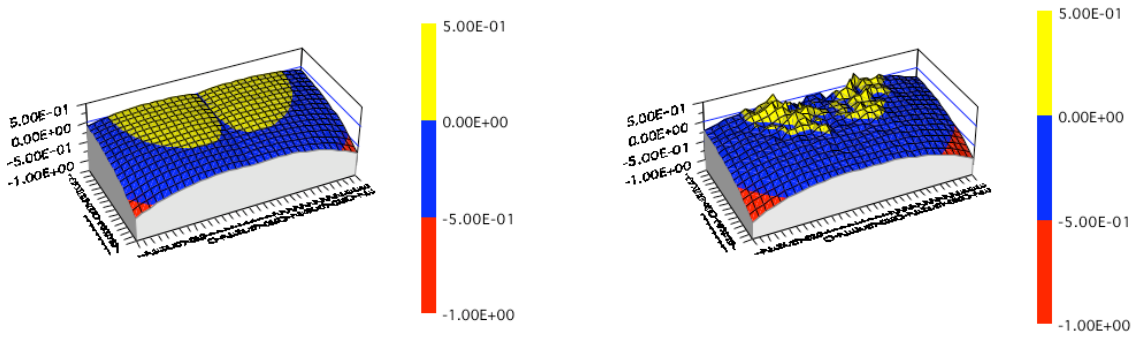

Fig. 3. Growth rate spectrum from Eq. (6). On the left is the growth rate of the linear instability. On the right is the growth rate in the saturated state.

Evaluation of Eq. (7) requires the values of $|n_k|^2$, $|\phi_k|^2$, and $\langle n_k^* \phi_k \rangle$ for the k_y = 0 part of the spectrum. In the saturated state, a closure theory described in the next section provides the stationary values of $|\beta_1|^2$, $|\beta_2|^2$, and $\langle \beta_1^* \beta_2 \rangle$, including those of zonal wavenumbers. Inverting the eigenmode decomposition, $n_k = R_1(k)\beta_1(k) + R_2(k)\beta_2(k)$ and $\phi_k = \beta_1(k) + \beta_2(k)$, then provides the needed correlations in the original fields. The saturation levels scale with the parameters of the original equations, from which the rate of finite amplitude-induced zonal mode damping is found to be $\gamma_k^{nl} = -\upsilon\varepsilon^{1/2}(1+k_x^2) / (1+k_x^2-\varepsilon^{1/2})$. This damping is as large as the growth rate, and present in modes that are preferentially driven by spectral transfer.

4. Saturation of TEM Turbulence

The preferential driving of zonal modes shown in Fig. 1, coupled with the robust nonlinear damping of zonal modes shown in Fig. 3, makes energy transfer to zonal modes the dominant saturation mechanism for collisionless TEM turbulence. This is demonstrated from measurement of spectral transfer rates in numerical solutions of the TEM equations and is shown in Fig. 4. The solid line plots $\mathrm{Re}(2i\omega_1)|\beta_1|^2$, the energy entering the unstable eigenmode from the linear instability. The broken line plots energy extracted from the unstable eigenmode via spectral transfer to the zonal modes. The near equality indicates that this transfer saturates the turbulence. There are other saturation channels, for example

spectral transfer within the unstable eigenmode to high wavenumber Fourier modes that are viscously damped. These channels play a minor role in saturation, unless the transfer to zonal modes is artificially removed in numerical calculations. In that situation, the fluctuation level must rise significantly to make these alternate channels sufficiently strong to balance the instability. This is illustrated in Fig. 5, which shows the evolution to steady state for a numerical solution in which zonal flow coupling is present versus one in which it is not. When the coupling is suppressed the fluctuation level rises by more than an order of magnitude.

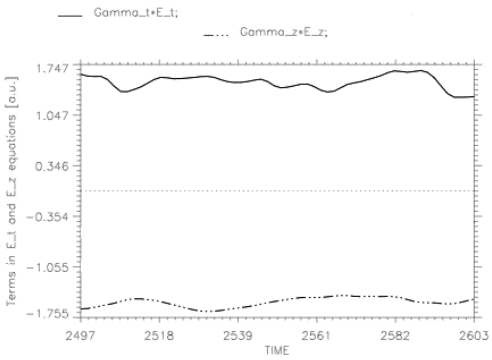

Fig. 4. Energy rates in the saturated state showing a balance between energy injected into the unstable eigenmode and energy transferred to zonal modes.

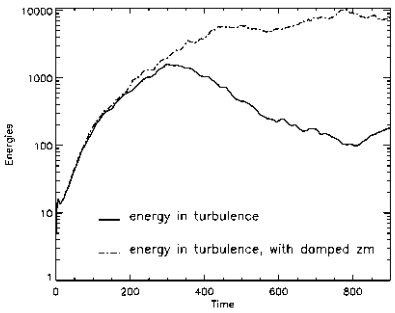

Fig. 5. Evolution of TEM turbulence for cases in which zonal mode coupling is artificially turned off (broken line) and present (solid line).

The energetics of Fig. 4, in which virtually all instability energy is transferred to zonal modes whose damping is as large as the growth rate, indicates that it is transfer to a sink that accounts for the lower fluctuation level in TEM when zonal modes are present. The lower saturation level is not a result of the shearing produced by zonal flows.

Analytic solution of Eq. (3) agrees with the results of Fig. 4. The solution requires a closure theory for the eigenmode energies $|\beta_1|^2$, $|\beta_2|^2$, $\mathrm{Im}\langle\beta_1^*\beta_2\rangle$, and $\mathrm{Re}\langle\beta_1^*\beta_2\rangle$, all of which contribute to the total fluctuation energy. Evolution equations for these energies in a self-consistent EDQNM closure are given in Ref. [8]. The closure equations are solved asymptotically for $\upsilon/k_y v_D \ll 1$, yielding the scaling of the energies with υ and $k_y v_D$. A separate asymptotic analysis with $\upsilon/k_y v_D \gg 1$ must be performed for the $k_y = 0$ zonal modes. These analyses show that the turbulent saturation levels are given by $|\beta_1|^2 \sim A_1 k_y^2 v_D^2$, $\mathrm{Im}\langle\beta_1^*\beta_2\rangle \sim A_i\, k_y^2 v_D^2\, (\upsilon/k_y v_D)$, $|\beta_2|^2 \sim A_2\, k_y^2 v_D^2\, (\upsilon/k_y v_D)^2$, and $\mathrm{Re}\langle\beta_1^*\beta_2\rangle \sim A_r\, k_y^2 v_D^2\, (\upsilon/k_y v_D)^2$, for $\upsilon/k_y v_D \ll 1$. These levels are set by dominant asymptotic balances with the spectral transfer terms that mediate the saturation balances. In the equation for $|\beta_1|^2$ a single spectral transfer term balances the growth rate at lowest order. This term transfers energy to the damped branch through $\mathrm{Im}\langle\beta_1^*\beta_2\rangle$. There are numerous Kolmogorov-like terms in which transfer is mediated by the coupling of three modes on the unstable branch. These terms carry energy to higher wavenumber, viscously damped Fourier modes on the unstable branch without coupling to modes of the damped branch. These terms are all subdominant. With the dominant saturation balance carrying energy to the damped branch, and with energy transfer subject to the anisotropy of Eq. (5), it is evident that the dominant saturation channel is via transfer to zonal modes of the damped eigenmode.

5. Inverse Spectral Energy Transfer

The dominant long wavelength nonlinearity $\nabla\phi\times\mathbf{z}\cdot\nabla n$ is known to produce transfer of energy to small scales [3]. It is thus important to determine how this nonlinearity can drive zonal modes at large scales. Even with the simplification of asymptotic analysis, the saturation balances beyond that of the $|\beta_1|^2$ equation are complicated. For example, in the $|\beta_2|^2$ equation the dominant balance includes nine separate terms involving different pairwise combinations of $|\beta_1|^2$, $|\beta_2|^2$, $\mathrm{Im}\langle\beta_1^*\beta_2\rangle$, and $\mathrm{Re}\langle\beta_1^*\beta_2\rangle$, and different combinations of wavenumber dependence on the wavenumbers k, k', and $k-k'$ of an interaction triad. To simplify the possibilities, spectral transfer terms are examined for special symmetries that facilitate inverse transfer.

Consider a rough antisymmetry property wherein spectral transfer terms change sign for $k\leftrightarrow k'$, without necessarily preserving magnitude [10]. This type of symmetry has been associated with inverse cascades in other systems. For example, the more restrictive case of exact antisymmetry (transfer terms preserve magnitude under $k\leftrightarrow k'$) yields the inverse cascade of mean squared flux in 2D MHD. The less restrictive condition of rough antisymmetry allows for inverse transfer in which the exchange between k and k' is not conservative, and other non-symmetric interactions are required to maintain energy conservation. Rough antisymmetry yields transfer that is either forward or inverse, depending on the sign of the transfer rate. For inverse energy transfer, the spectral transfer rate must be negative for $k<k'$. Looking at the spectral transfer rates of the dominant saturation balances described in the previous section, rough antisymmetry does not apply to the single spectral transfer term of the $|\beta_1|^2$ balance, but does apply to eight of the nine terms of the $|\beta_2|^2$ balance. Writing the $|\beta_2|^2$ equation as $[\partial/\partial t - 2\mathrm{Im}\omega_2]\,|\beta_2|^2 = -4\mathrm{Re}[T_{222}(k,k') + T_{122}(k,k')]$, the eight terms entering the dominant saturation balance with rough antisymmetry are in T_{222} and the other term is in T_{122}. Under general conditions T_{222} is complicated, with components producing both forward and inverse transfer, depending on spectrum shape. Inverse transfer dominates for a broad class of physically important spectra. Consider decaying spectra such that $|\beta_1|^2$, $|\beta_2|^2$, $\mathrm{Im}\langle\beta_1^*\beta_2\rangle$, and $\mathrm{Re}\langle\beta_1^*\beta_2\rangle$ have the same shape and fall off faster than k^{-1}. The spectra generated in numerical solutions of Eq. (3) belong to this class, as do the spectra of the canonical balance defining the wave-dominated regime [5], which go as k^{-2}. A broad transfer range is also assumed, such that energies at k are much larger than energies at k' for $k<k'$. In a wave dominated regime where linear wave frequencies exceed nonlinear wave frequencies, $T_{222}(k,k')$ is given by

$$2\mathrm{Re}T_{222}(k,k') = -\sum_{k'}\frac{(\mathbf{k}'\times\hat{\mathbf{z}}\cdot\mathbf{k}')^2(1-\varepsilon^{1/2})\upsilon}{v_D^2(1-\varepsilon^{1/2}\hat{\alpha})^3}\left[\frac{\upsilon\varepsilon^{1/2}(\hat{\alpha}-1)(1-\varepsilon^{1/2})}{v_D k_y^2(k_y-k_y')^2(1-\varepsilon^{1/2}\hat{\alpha})^2}\left|\beta_1''\right|^2\right.$$
$$\times\left[(k_y'-2k_y)\mathrm{Im}\langle\beta_1*\beta_2\rangle+(2k_y'-k_y)\mathrm{Im}\langle\beta_1'^*\beta_2'\rangle\right] + \left[k_y'\mathrm{Im}\langle\beta_1'^*\beta_2'\rangle - k_y\mathrm{Im}\langle\beta_1*\beta_2\rangle\right]$$
$$\left.\times\frac{\mathrm{Im}\langle\beta_1''^*\beta_2''\rangle}{k_y^3k_y'}\left[J_1(k_y-k_y')+J_2(k_y+k_y')\right]\right], \qquad (8)$$

where a shorthand notation has been adopted in which β_1 is understood to be evaluated at k, β_1' at k', β_1'' at $k-k'$; $J_1=-\left[1+(1/2)\hat{\alpha}\varepsilon^{1/2}(1+\varepsilon^{1/2})-2\varepsilon^{1/2}\right]$, and $J_2=(1/2)\hat{\alpha}\varepsilon^{1/2}(1-\varepsilon^{1/2})$. With one exception, all terms of Eq. (8) explicitly satisfy rough antisymmetry and produce inverse transfer, *i.e.*, they are negative for $k<k'$, and positive for $k>k'$. The constants J_1 and J_2 come from a single term. The J_1 piece is roughly antisymmetric. The J_2 piece is roughly symmetric and negative for all k. Hence it constitutes a source in β_2, fed by unstable β_1-modes. Consequently, once energy has been transferred to the damped eigenmode from the unstable eigenmode, its subsequent path in wavenumber space is governed by rough antisymmetry.

Equation (8) describes the transfer of energy from a short wavelength mode to a long wavelength mode, both of which belong to the damped eigenmode spectrum, with the mediation of a third unstable wave. The expression holds in a wave-dominated regime. The explicit condition for wave-dominated dynamics is a near-resonant condition on the damped eigenmodes at k and k' and the growing eigenmode at k-k'. The condition requires $i\omega_1(k\text{-}k') >> \Delta\omega_2(k')+\Delta\omega_2^*(k)$, where $\Delta\omega_2(k')$ and $\Delta\omega_2^*(k)$ are nonlinear frequencies induced by mode coupling. The closure theory gives an explicit expression for $\Delta\omega_2$ that is of order $v_D k_y$ [8]. This represents a significant shift from the linear frequency, which is of order $(\upsilon/v_D k_y)^2$. This prediction has been verified by comparison with direct numerical simulation. Using the expression for $\Delta\omega_2(k')+\Delta\omega_2^*(k)$ from the closure theory, the near resonant condition can be written,

$$\frac{v_D(k_y - k_y')(1-\varepsilon^{1/2}\hat{\alpha})^2}{[1+(k-k')^2-\varepsilon^{1/2}]} >> \sum_q \frac{\left[(\mathbf{k}'\times\hat{\mathbf{z}}\cdot\mathbf{q})^2-(\mathbf{k}\times\hat{\mathbf{z}}\cdot\mathbf{q})^2\right]|\beta_1(q)|^2(1+q^2-\varepsilon^{1/2})}{v_D q_y} . \qquad (9)$$

Dimensionally, this condition corresponds to the dominance of the wave frequency over the nonlinearity in Eq. (3). The regime in which this condition holds is analogous to the spectral subrange below the Rhines cutoff in quasigeostrophic turbulence [9] where spectral transfer is mediated by wave motion that is slow relative to motions of turbulence at small scales. Analysis of the closure theory expression for $\Delta\omega_2(k')+\Delta\omega_2^*(k)$ indicates that when Eq. (9) is not satisfied, the sign of T_{222} reverses and gives forward transfer. Near-resonant wave interactions have been implicated [11] in the inverse energy transfer of rotating [5] and rotating stratified turbulence [6], where otherwise the transfer is forward. Attempts to derive the relevant near-resonant condition have been frustrated by the limitations of the weak turbulence expansions that have been used in those analyses. Because the TEM system and those of rotating and rotating stratified turbulence behave similarly in so many ways [7], the present analysis and identification of responsible triads may shed light on the inverse transfer in those problems.

This work demonstrates the crucial role played by the damped eigenmode, and suggests that the full eigenmode spectrum should be considered in describing the long wavelength range of the spectrum where zonal modes form.

Work supported by USDOE

[1] LIN, Z., et al., Science **281** 1835 (1998).
[2] HASEGAWA, A., MIMA, K., Phys. Rev. Lett. **39** 205 (1977).
[3] NEWMAN, D.E., et al., Phys. Plasmas **1** 1592 (1994).
[4] JAKUBOWSKI, M, et al., Phys. Rev. Lett. **89** 265003 (2002).
[5] SMITH, L.M., WALEFFE, F., Phys. Fluids **11** 1608 (1999).
[6] SMITH, L.M. and F. Waleffe, J. Fluid Mech. **451** 145 (2002).
[7] TERRY, P.W., et al., Phys. Rev. Lett. **89** 205001 (2002).
[8] BAVER, D.A., et al., Phys. Plasmas **9** 3318 (2002).
[9] CHEKHLOV, A., et al., Physica **98D** 321 (1996).
[10] TERRY, P.W., "Inverse energy transfer by near-resonant interactions with a damped-wave spectrum", submitted, 2004.
[11] LEE, Y., Anisotropic Energy Transfer in β-Plane and Rotating Flows, PhD Thesis, Univ. of Wisconsin-Madison, Madison (2003).